

Freezing of water electrolyte confined in Nafion[®]

Membrane

Marie Plazanet,^{*,†} Renato Torre,[‡] Paolo Bartolini,[¶] Bruno Deme,[§] Caterina
Petrillo,^{||} and Francesco Sacchetti^{||}

*Laboratoire Interdisciplinaire de Physique, Universite Joseph Fourier et CNRS- UMR 5588,
BP87, 38402 Saint Martin d'Heres Cx, France, European Laboratory for Non-Linear
Spectroscopy (LENS) and Dip. di Fisica ed Astronomia, Università di Firenze, Via N. Carrara 1,
I-50019 Sesto Fiorentino, Firenze, Italy, European Laboratory for Non-Linear Spectroscopy
(LENS), Via N. Carrara 1, I-50019 Sesto Fiorentino, Firenze, Italy, Institut Laue langevin, BP 87,
38042 Grenoble Cx 9, France, and Dipartimento di Fisica, Università degli Studi di Perugia,
I-06123 Perugia, Italy*

E-mail: marie.plazanet@ujf-grenoble.fr

*To whom correspondence should be addressed

[†]LIPhy

[‡]LENS

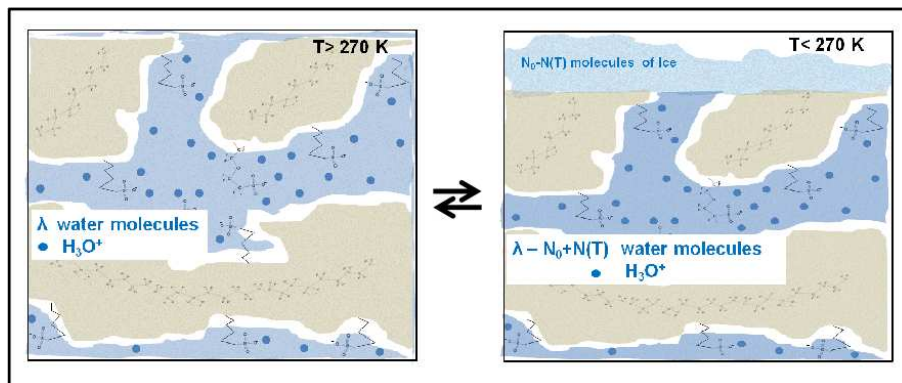
[¶]LENS

[§]ILL

^{||}Università di Perugia

Abstract

Water or electrolyte filled nano-structures are often encountered in soft condensed matter. An example is the Nafion[®] membrane, a particularly relevant system in which the confinement of water can be considered as model for electrolyte nano-confinement phenomena. This amphiphilic perfluorosulfonated polymer adopts a structural organisation made of channels and cavities, that water fills upon hydration. The sulfonate groups release the protons in water to form an electrolyte confined in the polymer matrix. The mechanism of water sorption/desorption and its connection with the temperature is still an open question. Performing neutron diffraction, we monitored the quantity of ice formed outside of the membrane as a function of temperature down to 180 K. The smooth and reversible behavior upon sorption or desorption of water is modelled on the basis of the freezing point depression of a solution. The quantitative agreement points out the origin of the phenomena, that could be more general in soft condensed systems.



Introduction

Hydration and dehydration of soft-condensed systems are complex processes that are the topics of many theoretical or experimental studies. Systems such as proteins, polymers or micellar surfactants exhibit often physico-chemical properties that depend on hydration. The hydration state may affect mechanical properties of hydrated polymers¹, structural organisation of surfactants², thermal fluctuations in proteins³, ionic conductivity of polymer membranes⁴... and the proper-

ties of water such as structure, freezing point or diffusion constants are affected by the interaction with the surrounding matrix and the presence of charges. Water properties continuously vary between two extreme states: from water strongly bound to the surface through hydrogen bonding, to nearly free water unaffected by the interaction with the (far enough) interface, therefore classified as bulk water. Several classes of water might be distinguished between these two cases: typically between 2 and 4 water populations may be defined depending on the experimental technique used to probe the state of water^{5,6}. The situation also depends on the presence of charges and on the water-matrix interactions⁷. Below 0°, the question of water crystallisation rises. Bound water does not crystallise, reaches an ultra viscous state and flows at temperatures of several tens of degrees below 0°C, enabling water transport at sub-zero temperature, an important phenomena for many applications. Bulk-like water crystallises either in the regular hexagonal form or in less common cubic phase⁸. The ice formation may strongly change the material properties, eventually leading to dehydration or damages. Getting a quantitative description of the water behaviour below 0°C is therefore of prime importance for many applications based on hydrogels or systems containing confined water, such as organisms cryopreservation, ion conducting membranes⁹ or food and drug industry¹⁰.

Particularly interesting systems are the perfluorosulfonated membranes: Nafion[®]¹¹ is a well known amphiphilic polymer made of fluorinated chains carrying hydrophilic sulfonate (SO_3^-) anions. It is widely used in a variety of applications, the best known being the use as proton conducting membranes in fuel cells¹². Its useful properties, related to the water structure and dynamics, are the result of a complex polymer organization in which the hydrophilic side chains are organized to form a network of channels and cavities that water fills upon hydration. The structure of the material and the dynamics of water are still a matter of debate and studies. Different structural models have been proposed, such as a percolating network of cavities and channels, an oriented nanochannels structure, or a random distribution of pores^{13–18}. The common feature to all of them is the presence of cavities formed by the sulfonate groups of characteristic dimensions of $\sim 2 - 6\text{ nm}$ depending on the amount of uptaken water. The water dynamics is also an important

issue due to its relation to the conductivity capabilities, and various diffusion mechanisms are proposed for the water and hydronium ions^{19–22}.

The organisation of the amphiphilic polymer leads to an aggregation of the anions to form hydrophilic charged cavities embedded in the hydrophobic matrix. These cavities can be filled with water, the amount of which, λ (λ = number of water molecules per sulfonate group), depends on temperature, Equivalent Weight (i.e. moles of sulfonate groups per grams of dry membrane) or heat treatment of the membrane^{23,24}. The dehydration of the membrane upon cooling below 0°C was first highlighted in the eighties^{25,26}, followed later by several more detailed studies^{27–34}. Pineri et al., see ref.³⁰, studied the water desorption mechanism and ice formation, and measured the time scales over which these processes take place. At temperature between 273 and 220 K, water maintains a mobility that enables the system to reach an equilibrium through desorption and ice formation on the membrane surface. Typically these kinetics are very slow, at 220 K the desorption process could take more than one hour in Nafion[®] 117 membranes of 175 μ thickness. Because of these slow kinetics, scanning calorimetric measurements are not suitable for the study of desorption process at low temperature, as equilibrium is not reached at the typical cooling rate used in such experiments. It was also reported that water crystallises and forms ice outside of the pores^{30,31}. But these observations have been contradicted by a recent study reporting that the water eventually crystallises inside a hyperswollen membrane in which the water content reached $\lambda \sim 50$ ³³: in this work, the freezing point depression of ice with respect to bulk water was interpreted in terms of confinement behaviour, where the melting point was determined accordingly to the Gibbs-Thomson equation of a liquid confined in a pore. Based on experimental data points recorded at discrete values of λ and T, the authors³³ favoured this interpretation rather than the effect of acidity on the freezing point.

Our previous study³¹ was based on the propagation of high frequency acoustic waves in a highly hydrated membrane ($\lambda \sim 30$) using optical Transient Grating (TG) spectroscopy. The detection of an acoustic wave propagating at the velocity of sound in ice was used to characterise the ice formation down to $\sim 220K$. The rather low acoustic damping proved the formation of microm-

eter size crystals, that can grow only outside of the membrane pores on the membrane surface. The amount of external ice follows a surprisingly smooth and continuous behaviour as a function of temperature, both on cooling and heating. The amount of ice formed could be modelled by a power law of the difference $(T - T_c)$, T_c being the pseudo-critical temperature below which the ice phase exists. This behavior indicates that the phenomenon is not simply related to the freezing of confined water, as previously proposed^{33,35}, but is indeed related to a more complex mechanism involving the desorption/sorption processes.

Experimental Results

In order to further investigate the origin of these processes, we performed a Neutron Diffraction investigation. Using D_2O hydrated membranes, we were able to quantitatively monitor the ice formation over an extended temperature range, providing information on the structural features of the ice crystallites and the Nafion membrane. The sample with a water content of $\lambda \sim 40$ was prepared according to the procedure reported in the "Material and Methods". The Bragg peak intensities are directly related to the amount of ice. The measurements were performed on complete temperature cycles, with waiting times longer than 20 minutes between measurement points separated by 10 degrees, in order to reach equilibrium. Diffraction patterns measured during cooling and heating are shown in 1 and exhibit changes in the peak intensities down to ~ 180 K. This range of temperatures over which water mobility is observed is in agreement with measurements of mechanical properties³⁴ that show an elastic energy dissipation due to unfrozen water down to 180 K. The instrument-limited width of Bragg peaks indicates that the crystals are larger than the typical pore sizes, so they must grow outside of the membrane pores. A rough estimate based on Scherrer's equation³⁶ indicates indeed a size of crystallites larger than 10 nm, in agreement with the micrometer size previously estimated. Within the diffractometer resolution and with reasonable assumption for crystals of fairly large size, we can check that the ice crystallises in the common hexagonal form (Ih). Because of the percolating network of water channels in the polymer, the ice crystallites

formed on the membrane surface are in contact with the liquid fractions of water remaining inside the polymer matrix, the two phases being in thermodynamical equilibrium but governed by two different chemical potential.

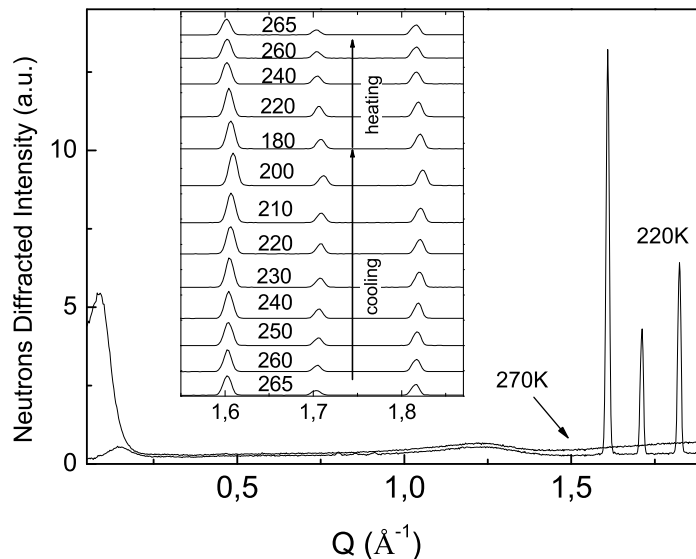


Figure 1: Diffraction patterns measured on D16 (ILL) at room temperature and 220 K. The inset shows the three peaks characteristics of hexagonal ice as a function of temperature upon cooling and heating.

The diffraction results confirm previous observations from optical TG experiments³¹, with an overall temperature shift of a few degrees due to the fact that D_2O was used for neutron experiment while H_2O was used in the optical experiments. The inset of 1 represents the temperature evolution of the intensities of the three Bragg peaks characteristic of ice Ih at momentum transfer of about 1.6 Å^{-1} (100), 1.7 Å^{-1} (002) and 1.8 Å^{-1} (101). Like in our previous experiments³¹, using TG spectroscopy and X-ray diffraction, a small hysteresis is observed in ice formation. The ice appears only about 6-7 degrees below the melting point of bulk ice upon cooling, and can be monitored up to about 2 degrees below the melting point upon heating.

Beside the Bragg peaks arising from ice formation, the sorption/desorption of water is also reflected in the position of the matrix ionomer peak at $\sim 0.12 \text{ Å}^{-1}$ as shown in 2. The position of this peak is well documented¹⁵ and depends on the hydration of the membrane. The shift,

measured here as a function of temperature, follows the same trend as it does upon the variation of hydration level at room temperature. The quite low position of the peak (0.08 \AA^{-1}) at room temperature also confirms the high hydration level determined from membrane weighting.

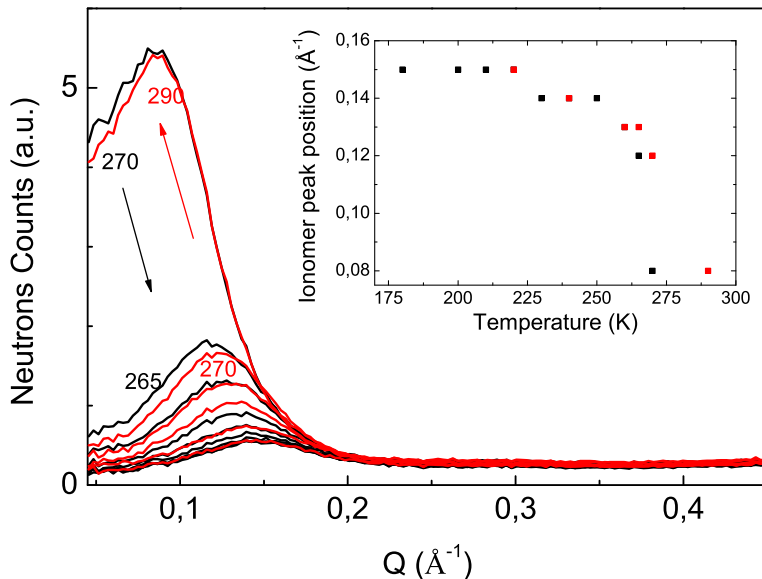


Figure 2: Small angle part of the diffraction pattern, showing the ionomer peak region as a function of temperature. The inset shows the variation of the position of the peak during the temperature cycle. The hysteresis can be seen around 275 K

This behaviour can be assigned to the difference of chemical potential of water inside the membrane (therefore the one of a liquid solution) and outside the membrane (regular ice) smoothly varying with temperature. This difference provides the energetic contribution driving the water in and out of the membrane, which is, in other terms, an osmotic pressure. Based on the electrolyte nature of the polymer, we consider that the liquid confined in the cavities is a solution of hydronium ions in water. We therefore describe the continuous variation of the quantity of ice in the sample with temperature by the solution behaviour, in which the freezing point depends on the solute concentration and therefore varies with hydration. At the freezing point of the solution, the most favourable process is to expel water out of the membrane, increasing the concentration of the hydronium ions inside the membrane. The water crystallises therefore following a first order transition spread over a wide temperature range. Considering a model of ideal solution, the melting

point depression is related to the solute fraction x_s (mol solute / (mol of solute + mol of water)) by the equation³⁷:

$$\ln(1 - x_s) = \frac{\Delta H_{fus}}{R} \cdot \left(\frac{1}{T_0} - \frac{1}{T} \right) \quad (1)$$

where R is the gas constant, T_0 is the bulk melting point of the pure liquid and ΔH_{fus} the enthalpy of fusion of ice. $T_0 = 277.15$ for D_2O , and the temperature dependence of ΔH_{fus} is taken from reference³⁸, and shifted by 292 J/mol for D_2O . The diffracted intensity I is proportional to the number of crystallised water molecules, and is normalised to 1 at the lowest temperature. I can therefore be written as:

$$I(T) = \frac{1}{N_0} [N_0 - N(T)] \quad (2)$$

where N_0 is the number of desorbing water molecules at the lowest temperature, and $N(T)$ is the number of water molecules that participate to the solution above a given temperature and desorb below. $N(T)$ is related to the solute fraction $x_s(T)$, as follows: $x_s(T) = 1/(1 + N(T))$. 3 represents the average of the integrated intensities of the three diffraction peaks as a function of temperature together with the calculated intensities as described above.

As stated in the introduction, several classes of water molecules can be distinguished in such systems, due to the interaction with the polymer surface (*freezing bound* water^{7,25}), and the hydration shell of the hydronium ions³⁸. Therefore not all water molecules present in the sample but only a fraction of them participate in the ice formation process. To take these water populations into account, N_0 is an adjustable parameter. If all water molecules crystallised, N_0 would equal the hydration level λ , therefore $N_0 \sim 40$.

In fact, the number of $N_0 = 25$ gives the best fit to the experimental data. This indicates an averaged number of 15 water molecules that do not crystallise at any temperature. Most studies show a minimum number of $\lambda \sim 8$ molecules that do not crystallise due to interaction with the cavity surfaces, reducing the amount of free water to be considered in the behaviour of the solution³⁸. Moreover, considering the complexity of the membrane structure, not all water molecules λ are

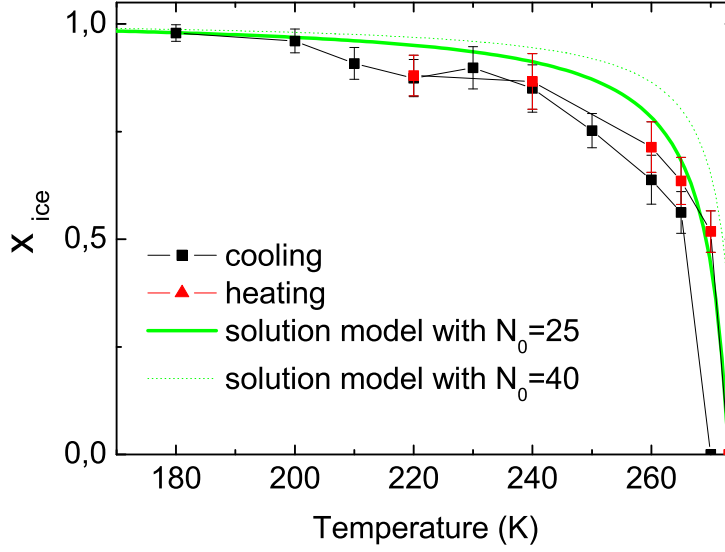


Figure 3: Temperature dependence of the integrated intensity of the three diffraction peaks at 1.6, 1.7 and 1.8 \AA^{-1} , normalised to 1 at the lowest temperature. Solid line represents the intensity of an ideal solution in which the total number of crystallising water molecules equals 25. The dotted line represents the same calculation with $N_0=40$.

necessarily trapped in cavities and give rise to water desorption: the amount of water available for desorption reduces further. This observation is also in agreement with measurements by the group of G. Gebel, in which no crystallisation is observed below $\lambda = 18$ ³³.

The diffracted intensity, reached when the ice eventually appears around 265 K, is within experimental uncertainties the same as measured upon heating. This indicates that the hysteresis observed between ice formation upon cooling and ice melting is only a temperature delay. This argument is in favour of capillary freezing-hysteresis, which is indeed currently observed in porous media³⁹.

The confrontation of the solution model proposed in this work with the previous Transient Grating data reported in reference³¹ is shown in 4. The solution model introduced in this work is also in very good agreement also with data measured in this previous work³¹. Indeed, the TG amplitudes are directly proportional to the amount of ice formed outside the membrane and its temperature dependence can therefore be described by the solution model. The fit of the power law,

previously proposed, is also reported for comparison between the two models, and is compatible with the data only in a restricted range of temperatures.

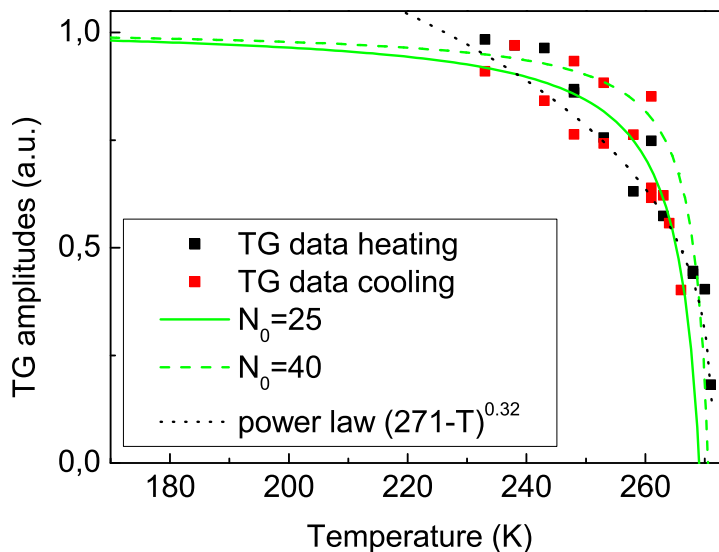


Figure 4: Amplitudes of the TG data reported in Ref.³¹. As in 3, the solid line represents the amplitude from an ideal solution with $N_0 = 25$. The dotted line represents the same calculation with $N_0=40$. The black dotted line represent the fit with the phenomenological power law previously proposed.

We therefore propose that the main driving mechanism for water sorption/desorption in the Nafion membrane at low temperature is due to the electrolyte behaviour.

Discussion

Although confined electrolyte are ubiquitous in nature, the conditions to have reversible water desorption below 0 °C are not well established. The amount of freezing and non-freezing water depends on several factors, like the ionic nature of the solution, the porosity, the mechanical properties of the matrix or the water-matrix interactions^{40–44}. Non freezing water, or water sorption and desorption has been observed in several systems as discussed below, but Nafion is, to our best knowledge, the first polymeric system in which low temperature water transport has been ob-

served. Based on the phenomena observed in the Nafion material, H. Mendil-Jakani et al. checked the behaviour of water-saturated sulfonated polyimide membranes. Despite electrolyte properties similar to those of the Nafion polymer, no water desorption was observed. They assigned this fact to the strong interaction between water and polymer groups, maintaining the water inside the membrane³³. Water properties have also been extensively studied in biocompatible polymers, where the structure of water close to the surface of the polymer is believed to be a major factor for biocompatibility^{6,45}. However, due to the slow kinetics, studies based on DSC measurement do not provide all information necessary for the understanding of the nature of the water confined in polyelectrolytes. Only few systems have been studied using different techniques, and desorption effects have not been emphasised yet.

Another typical example of soft confinement is given by hydrated surfactant. Water in oil reverse micelles of typically 1-5 nanometers core diameter, formed by the charged surfactant AOT, supercooled water is observed down to several tens of Kelvin. But the ideal solution behaviour, considered to explain the freezing point depression, did not justify the large depressions observed in these experiments⁴⁶. Nonetheless, surfactants forming lamellar phases separated by interstitial water seem to exhibit ultra viscous water: the water confined in model lipid membranes made of charged surfactants is also transported in and out of the layers at sub-zero temperatures⁴⁷, forming ice pools in contact with the non-freezing interstitial water. As in the Nafion case, the ice formation gradually increases upon temperature decrease, in a reversible way, with a little hysteresis assigned to water supercooling. The same effect has been observed in the natural Purple Membrane^{48,49}, between 250 and 273 K. The kinetics of water migration in and out of the interlamellar spaces were evidenced, with timescales similar to those measured in Nafion. Extensive studies of water transport in flash-cooled portein crystals have been conducted with the aim of improving the quality of crystallographic data. The crystals are usually quenched to low temperature and annealing cycles are then performed between 100 and 273 K. During the annealing phases and around 230-250 K, depending on the environmental humidity, liquid-like water is observed to be transported in and out of the crystals⁵⁰⁻⁵². Eventually, montmorillonite, a silicate based clay in which water

is confined together with various cations, also exhibits the same phenomena⁵³.

Although most of the systems previously cited contain charges, various interpretations have been proposed for the freezing point depression of confined water: confinement effect governed by the Gibbs-Thompson equation, osmotic pressure or disjoining pressure. Further studies on other model systems containing confined water with different physico-chemical properties would therefore be necessary to clarify the relevant parameters relative to the observation of reversible water desorption below 0 °C.

Materials and Methods

Sample preparation. Nafion 112[®] was purchased from Ion Power Inc. (USA), and the sample was prepared according to the same procedure described in³¹. After cleaning, the membranes were rinsed and boiled several times in D_2O . Careful weighing of the sample enabled the determination of $\lambda \sim 40$. The membranes were then cooled to liquid nitrogen temperature and ground, in order to get a powder of millimeter size grains and to ensure good orientational averaging in neutron diffraction experiment. The membrane itself has a thickness of 54 μ .

Neutron scattering experiment. Neutron diffraction was performed in the Q-range of 0.02 – 2.0 \AA^{-1} on the small momentum transfer diffractometer D16 (ILL, Grenoble, France), using a wavelength of 4.75 \AA and an angular range of $[2 - 125^\circ]$. The sample was placed in a cryostat with quartz windows and the temperature was controlled to within 0.1 K. D_2O hydrated samples were used in order to decrease the incoherent background arising from hydrogen atoms and to increase the coherent scattering at the origin of the diffraction pattern.

Acknowledgements

This work was supported by REGIONE TOSCANA POR-CRO-FSE 2007-2013 by EC COST Action MP0902-COINAPO. We would like to thank A.Taschin for his support on TG experiments.

References

- (1) Zhao, Q; Benziger, J. *J. Polym. Sci.: Polym. Phys.* **2013**, 23284.
- (2) Kotlarchyk, M.; Chen, S.-H.; Huang, J.S.; Kim M. W. *Phys. Rev. Let.* **1984**, 53, 941.
- (3) Reat, V.; Patzelt, H.; Ferrand, M.; Pfister, C.; Oesterhelt, D.; Zaccari, G. *Proc. Natl. Acad. Sci. USA* **1998**, 95, 4970-4975.
- (4) Hickner, M.A. *J. Polym. Sci. B: Polym. Phys* **2012** 50, 9-20.
- (5) Corkhill, P.H.; Jolly, A.M.; Ng, C.O.; Tighe, B. *J. Polymer* **1987** 28, 1758-1766.
- (6) Pissis, P.; Kyritsis, A. *J. Polym. Sci. B: Polym. Phys.* **2013**, 51, 159-175.
- (7) Hatakeyama, T.; Tanaka, M.; Kishi, A.; Hatakeyama, H. *Acta Biomater.* **2010**, 6, 2077-2082.
- (8) Hansen, T. C.; Koza, M. M.; Kuhs, W.F. *J. Phys. Cond. Mat.* **2008**, 20, 285104.
- (9) Neburchilov, V.; Martin, J.; Wang, H.; Zhang, J. *J. Pow. Sources* **2007**, 169, 221-238.
- (10) Zohuriaan-Mehr, M.J.; Pourjavadi, A.; Salimi, H.; Kurdtabar, M. *Polym. Adv. Technol.* **2009**, 20, 655-671.
- (11) DupontTM Nafion Membranes.
- (12) Dupuis, A.-C. *Prog. Mat. Sci.* **2011**, 56, 289-327.
- (13) Gierke, T. D.; Munn, G. E.; Wilson, F.C. *J. Polym. Sci. Polym. Phys. Ed.* **1981**, 19, 1687-1704.
- (14) Hsu, W. Y.; Gierke, T. D. *J. Membr. Sci.* **1983**, 13, 307.
- (15) Gebel, G. *Polymer* **2000**, 41, 5829-5838.
- (16) Rollet, A.-L.; Diat O.; Gebel, G. *J. Phys. Chem. B* **2002**, 106, 3033-3036.
- (17) Mauritz, K.A.; Moore, R.B. *Chem. Rev.* **2004**, 104, 4535.

- (18) Schmidt-Rohr, K.; Chen, Q. *Nat. Mater.* **2008**, 7, 75-83.
- (19) Choi, P.; Jalani, N.H.; Datta, R. *J. Electrochem. Soc.* **2005**, 152, E123-E130.
- (20) Paciaroni, A.; Casciola, M.; Cornicchi, E.; Onori, G.; Pica, M.; Narducci, R. *J. Phys. Chem. B* **2006**, 110, 13769.
- (21) Perrin, J.-C.; Lyonnard, S.; Volino, F. *J. Phys. Chem. C* **2007**, 111, 3393-3404.
- (22) Feng, S.; Voth, G.A. *J. Phys. Chem. B* **2011**, 115, 5903-5912.
- (23) Maldonado, L.; Perrin, J.-C.; Dillet, J.; Lottin, O. *J. of Memb. Sci.* **2012**, 389, 43-56.
- (24) Choi, P.; Jalani, N.H.; Datta, R. *J. Electrochem. Soc.* **2005**, 152, E84-E89.
- (25) Escoubes, M.; Pineri, M.; Robens, E. *Thermochim. Acta* **1984**, 82, 149-160.
- (26) Pineri, M.; Volino, F. *J. Polym. Sci.: Polym. Phys.* **1985**, 23, 2009-2020.
- (27) Yoshida, H.; Miura, Y. *J. Memb. Sci.* **1992**, 68, 1-10.
- (28) Corti, H.R.; Norez-Pondal, F.; Pilar Buera, M. *J. Power Sources* **161**, 799 (2006).
- (29) Thompson, E.L.; Capehart, T.W.; Fuller, T.J.; Jorne, J. *J. Electrochem. Soc.* **2006**, 153, A2351-A2362.
- (30) Pineri, M.; Gébel, G.; Davies, R.J.; Diat, O. *J. Power Sources* **2007**, 172, 587-596.
- (31) Plazenet, M.; Barolini, P.; Torre, R.; C. Petrillo, C.; Sacchetti, F. *J. Phys. Chem. B* **2009**, 113, 10121-10127.
- (32) Guillermo, A.; Gébel, G.; Mendil-Jakani, H.; Pinton, E. *J. Phys. Chem. B* **2009**, 113, 6710-6717.
- (33) Mendil-Jakani, H.; Davies, R.J.; Dubard, E.; Guillermo, A.; Gébel, G. *J. Membrane Sci.* **2011**, 369, 148-154.

- (34) Teocoli, F.; Paolone, A.; Palumbo, O.; Navarra, M.A.; Casciola M.; Donnadio, A. *J. Polym. Sci. B* **2012**, 50, 1421-1425.
- (35) Sivashinsky N.; Tanny, G.B. *J. Appl. Polym. Sci.* **1981**, 26, 2625-2637.
- (36) Patterson, A.L. *Phys. Rev.* **1939**, 56, 978.
- (37) Laidler, K. J.; Meiser, J. H. *Physical Chemistry*, 2nd ed.; Houghton Mifflin: Boston, MA, 1995; Chapter 5.
- (38) Zavitsas, A.A. *Chem. Eur. J.* **2010**, 16, 5942-5960.
- (39) Christenson, H.K. *J. Phys.: Cond. Mat.* **2001**, 13, R95-R133.
- (40) Semenova, S.I.; Ohya, H.; Soontarapa, K. *Desalination* **1997**, 110, 251-286.
- (41) Chan, K.; Hirotsu, T.; Hatakeyam, T. *Eur. Polym. J.* **1992**, 28, 1021-1025.
- (42) Kusumocahyo, S.P.; Sano, K.; Sudoh, M.; Kensaka, M. *Separation and Purification Technology* **2000**, 18, 141-150.
- (43) Ostrowska-Czubenko, J. ; Gierszewska-Druzynska, M. *Carbohydrate Polym.* **2009**, 77, 590-598.
- (44) Amnuaypanich, S. Patthana, J.; Phinyocheep, P. *Chem. Eng. Sci.* **2009**, 64, 4908-4918.
- (45) Hatakeyama, T.; Tanaka, M.; Hatakeyama, H. *Thermochim. Acta* **2012**, 532, 159-163.
- (46) Spehr, T.; Frick, B.; Grillo, I.; Stuhn, B. *J. Phys. Cond. Mat. B* **2008**, 20, 104204.
- (47) Gleeson, J.T.; Erramilli, S.; Gruner, S.M. *Biophys. J.* **1994**, 67, 706-712.
- (48) Weik, M.; Lehnert U.; Zaccai, G. *Biophys. J.* **2005**, 89, 3639-3646.
- (49) Lechner, R.E.; Fitter, J.; Dencher, N.A.; Hauss, T. *J. Mol. Biol.* **1998**, 277, 593-603.

- (50) Weik, M.; Schreurs, A.M.M.; Leiros, H.-K.S.; Zaccai, G.; Ravelli, R.B.G.; Gros, P. *J. Synchrotron Rad.* **2005**, 12, 310-317.
- (51) Kriminski, S.; Caylor, C.L.; Nonato, M.C.; Finkelsteinc, K.D.; Thorne, R.E. *Acta Cryst. D* **2002**, 58, 459-471.
- (52) Juers, D.H.; Matthews, B.W. *Acta Cryst. D* **2004**, 60, 412-421.
- (53) Anderson D.M. *J. Coll. Interf. Sci.* **1967**, 25, 1714-191.